

Spitzer 24micron Observations of Optical/Near-IR Selected Extremely Red Galaxies: Evidence for Assembly of Massive Galaxies at $z \sim 1 - 2$?

Lin Yan¹, Philip I. Choi¹, D. Fadda¹, F.R. Marleau¹, B.T. Soifer^{1,2},
M. Im³, L. Armus¹, D.T. Frayer¹, L.J. Storrie-Lombardi¹, D.J. Thompson², H.I. Teplitz¹,
G. Helou¹, P.N. Appleton¹, S. Chapman², F. Fan¹, I. Heinrichsen¹, M. Lacy¹, D.L. Shupe¹,
G.K. Squires¹, J. Surace, G. Wilson¹

ABSTRACT

We carried out the direct measurement of the fraction of dusty sources in a sample of extremely red galaxies with $(R - K_s) \geq 5.3\text{mag}$ and $K_s < 20.2\text{mag}$, using $24\mu\text{m}$ mid-infrared data from the *Spitzer Space Telescope*. Combining deep $24\mu\text{m}$, K_s - and R -band data over an area of $\sim 64\text{ sq. arcmin}$ in the ELAIS N1 field of the Spitzer First Look Survey (FLS), we find that $50 \pm 6\%$ of our ERO sample have measurable $24\mu\text{m}$ flux above the 3σ flux limit of $40\mu\text{Jy}$. This flux limit corresponds to a SFR of $12M_\odot/\text{yr}$ at $z \sim 1$, much more sensitive than any previous long wavelength measurement. The $24\mu\text{m}$ -detected EROs have 24-to-2.2 and 24-to- $0.7\mu\text{m}$ flux ratios consistent with infrared luminous, dusty sources at $z \geq 1$, and an order of magnitude too red to be explained by an infrared quiescent spiral or a pure old stellar population at any redshift. Some of these $24\mu\text{m}$ -detected EROs could be AGN, however, the fraction among the whole ERO sample is probably small, 10-20%, as suggested by deep X-ray observations as well as optical spectroscopy. Keck optical spectroscopy of a sample of similarly selected EROs in the FLS field suggests that most of the EROs in ELAIS N1 are probably at $z \sim 1$. The mean $24\mu\text{m}$ flux ($167\mu\text{Jy}$) of the $24\mu\text{m}$ -detected ERO sample roughly corresponds to the rest-frame $12\mu\text{m}$ luminosity ($\nu L_\nu(12\mu\text{m})$) of $3 \times 10^{10}L_\odot$ at $z \sim 1$. Using the correlation between IRAS $\nu L_\nu(12\mu\text{m})$ and infrared luminosity $L_{IR}(8 - 1000\mu)$, we infer that the $\langle L_{IR} \rangle$ of the $24\mu\text{m}$ -detected EROs is $3 \times 10^{11}L_\odot$ and $10^{12}L_\odot$ at $z = 1.0, 1.5$ respectively, similar

¹Spitzer Space Telescope Science Center, California Institute of Technology, 1200 East California Boulevard, MS 220-6, Pasadena, CA 91125; Send offprint requests to Lin Yan: lyan@ipac.caltech.edu.

²The Caltech Optical Observatories, Caltech, Pasadena, CA 91125

³School of Earth and Environmental Sciences, Seoul National University, Shillim-dong, Kwanak-gu, Seoul, S. Korea

to that of local LIRGs and ULIGs. The corresponding SFR would be roughly $50 - 170 M_{\odot}/\text{yr}$. If the time scale of this starbursting phase is on the order of 10^8yr as inferred for the local LIRGs and ULIGs, the lower limit on the masses of these $24\mu\text{m}$ -detected EROs is $5 \times 10^9 - 2 \times 10^{10} M_{\odot}$. It is plausible that some of the starburst EROs are in the midst of violent transformation to become massive early type galaxies at the epoch of $z \sim 1 - 2$.

Subject headings: galaxies: bulges – galaxies: starbursts – galaxies: infrared luminous – galaxies: galaxy evolution – galaxies: high-redshifts

1. Introduction

Optical/near-IR colors, such as $(R - K_s)$ or $(I - K_s)$ have been commonly used in wide-area surveys to select old stellar populations at $z \sim 1 - 2$ (Cimatti et al. 2002; McCarthy et al. 2001; McCarthy 2004 for the review of this subject). Near-IR observations, which sample cool low-mass stars, are sensitive to old stellar populations. The $(R - K_s)$ of 5.3 corresponds to the calculated color of a passively evolving elliptical galaxy at $z = 1$. Therefore, in principle, the color criterion of $(R - K_s) \geq 5.3 \text{mag}$ or $(I - K_s) \geq 4 \text{mag}$ (EROs) should select early type galaxies at $z \sim 1$. However, these color selections are also sensitive to dust-reddened, star-forming systems, and examples of both passively evolving ellipticals and dusty starburst EROs have been found (Soifer et al. 1999; Hu & Ridgway 1994; McCarthy, Persson & West 1992; Graham & Dey 1996). This indicates that the optical/near-IR SEDs of these sources are sufficiently degenerate that these color criteria cannot effectively distinguish between them. In addition, a small fraction of EROs (10-20%) could also be AGN, as shown by deep Chandra data and optical spectroscopy (Alexander et al. 2002; Yan, Thompson & Soifer 2004). The relative contribution of these two galaxy types — old stellar populations and dust-reddened, star-forming galaxies — is a critical issue for many surveys whose goal is to determine the evolution of the mass function and the formation of massive galaxies. Deep optical spectroscopy indicates that a large fraction (30-50%) of EROs have emission lines (Cimatti et al. 2002; Yan, Thompson & Soifer 2004; McCarthy et al. 2004); however, it remains unclear what fraction of EROs are truly dust obscured galaxies.

MIPS $24\mu\text{m}$ data from the *Spitzer Space Telescope* (Rieke et al. 2004; Werner et al. 2004) offer the first opportunity to directly address this critical issue. Dusty, star-forming galaxies are clearly distinguished from early-type galaxies at mid-IR wavelengths. Between $z \sim 1 - 2$, the MIPS data is especially discriminating as strong, rest-frame 6–12 μm polycyclic aromatic hydrocarbon (PAH) dust features redshift into the $24\mu\text{m}$ -band. In this Letter, we present our initial study of the $24\mu\text{m}$ properties of the $(R - K_s \geq 5.3) \text{mag}$ selected EROs

in the ELAIS N1 field. Throughout the paper, we adopt $H_0 = 70\text{kms/s/Mpc}$, $\Omega_M = 0.3$, $\Omega_\Lambda = 0.7$, and the Vega system for optical/NIR magnitudes.

2. Data

2.1. Spitzer $24\mu\text{m}$ Observations and Data Reduction

The primary dataset used in this Letter is in the ELAIS N1 field, which is a part of the Spitzer First Look Survey (FLS)⁴. The field was observed in a 2×2 photometry mode mosaic, and the raw data were processed and stacked by the data processing pipeline at the Spitzer Science Center (SSC). Source catalogs at $24\mu\text{m}$ were generated using StarFinder (Diolaiti et al. 2000), which measures profile-fitted fluxes for point sources. The complete description of the $24\mu\text{m}$ data reduction and source catalog can be found in Fadda et al. (2004b) and Marleau et al. (2004). To aid in the interpretation of the results from ELAIS N1, we also analysed the FLS verification strip (FLSV). The data presented here covers 64 sq.arcmin in ELAIS N1 and 256 sq.arcmin in the FLSV. Table 1 summarizes the salient characteristics of all data used in this paper.

2.2. Optical, Near-IR Imaging and Keck Spectroscopy

All R -band observations were taken with the MOSAIC-1 camera on the 4m telescope at the Kitt Peak National Observatory. Reduced and stacked images as well as source catalogs have been publicly released; for details, see Fadda et al. (2004a). The K_s -band data were obtained using the Wide-Field Infrared Camera (WIRC) on the Palomar 200-inch telescope. The Elais N1 observations were taken in a single, deep $8' \times 8'$ pointing. A detailed description of the WIRC observations and data reduction will be included in a separate paper by Choi et al. (2004). Finally, high-resolution, optical spectra of a K_s -selected galaxy sample within the FLS region were obtained using the Keck, Deep Imaging Multi-Object Spectrograph (DEIMOS) (Faber et al. 2003). A total of ≈ 1000 redshifts were measured, of which 112 (52 EROs) are included in the analysis in this paper.

⁴For details of the FLS observation plan and the data release, see <http://ssc.spitzer.caltech.edu/fls>.

3. Results and Implications

3.1. The $24\mu\text{m}$ detected EROs

Since the R - and K_s -band data have similar seeing, $(R - K_s)$ colors were measured using a fixed $3''$ diameter aperture. The ERO catalog with $(R - K_s) \geq 5.3\text{mag}$ and $K_s < 20.2\text{mag}$ (6σ) consists of 129 galaxies over 64 sq.arcmin in ELAIS N1. Figure 1 shows the $(R - K_s)$ vs. K_s distribution for all sources (*black crosses*). The $(R - K_s) \geq 5.3\text{mag}$ and $K_s < 20.2\text{mag}$ limits are shown as *solid horizontal* and *solid vertical lines*, and sources with $24\mu\text{m}$ detected counterparts are indicated as *red open circles*. We find that $24\mu\text{m}$ detected sources have slightly redder $(R - K_s)$ colors than non-detected sources, consistent with the expectation that $24\mu\text{m}$ emission is an indicator of dust extinction.

To merge the R/K and $24\mu\text{m}$ source catalogs, we used a simple positional matching method with a $2.4''$ match radius, which corresponds to 3σ combined astrometric uncertainty from the K_s and $24\mu\text{m}$ data. Due to the relatively low source density (7arcmin^{-2}), the likelihood of spurious matches is small (3%), consistent with the fact that we find only one multiple match out of 65. In addition, we test the robustness of each match by comparing the probability of the measured separation based on the astrometric uncertainties to the probability of a spurious detection based on the $24\mu\text{m}$ source density. The probability ratios above unity imply to be likely real matches, and we found that all but two matches meet this criteria. We retained these two matches since the visual inspection suggests that they could still be associated with physical offset centroids. In addition, bright stars were rejected using R -band images. Stellar contamination in our sample is expected to be small since the field is at the galactic latitude of 41° , and $24\mu\text{m}$ data samples the tail of the Rayleigh-Jeans energy distribution.

Of the 129 EROs, 65 ($50 \pm 6\%$) have $24\mu\text{m}$ emission with flux greater than $40\mu\text{Jy}$. The fraction of $24\mu\text{m}$ detected EROs becomes slightly higher for redder sources, with $56 \pm 15\%$ and $67 \pm 30\%$ for $(R - K_s) \geq 6.0\text{mag}$ and $(R - K_s) \geq 6.5\text{mag}$ respectively. However, the errors of these fractions are large due to the shallow R band limit. Deeper data would be needed to reduce the uncertainties. In figure 2a, we show the $24\mu\text{m}$ flux distributions of both the total and ERO samples. We find that 70% of the $24\mu\text{m}$ EROs have $f_{24\mu\text{m}} > 90\mu\text{Jy}$ and that the mean $24\mu\text{m}$ flux of the ERO sample is $167\mu\text{Jy}$. Figure 2b shows K_s vs. $24\mu\text{m}$ flux for all detected sources (*solid squares*) and for the EROs (*large open circles*). We find that amongst the $24\mu\text{m}$ detected sources, K_s is weakly correlated with $f_{24\mu\text{m}}$, with large scatter. This is expected since these two bands sample light from different physical origins, stellar photosphere versus dust emission. This also explains why many faint K_s sources have fairly bright $24\mu\text{m}$ fluxes. For K_s bright ($\sim 18 - 17$) and $24\mu\text{m}$ -faint sources, the mid-infrared

data is deep enough to detect the emission from normal galaxy populations at low redshifts.

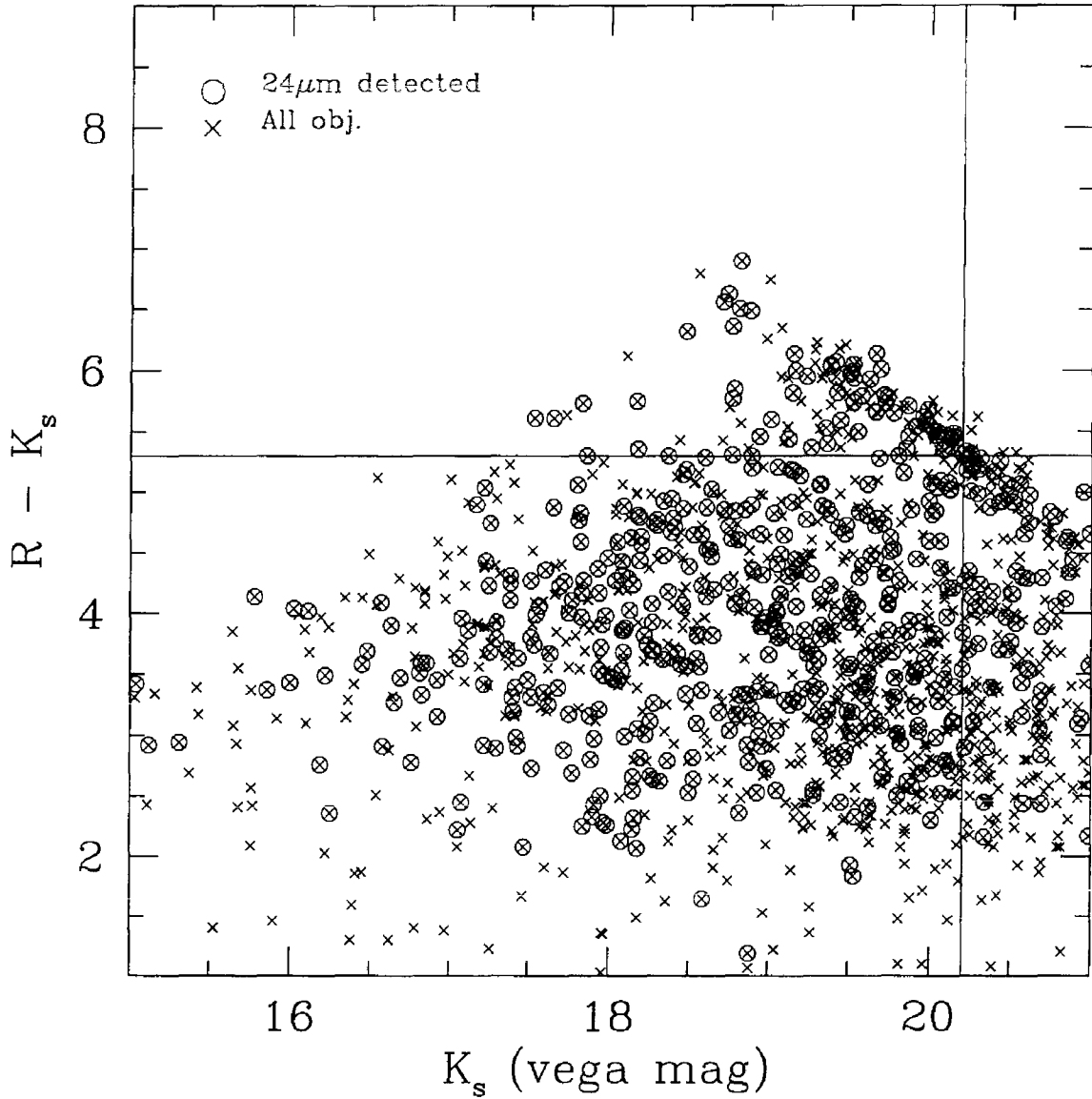


Fig. 1.— The $(R - K_s)$ vs. K_s color-magnitude diagram. All K_s -band detected sources are shown as *crosses*, and sources with $24\mu\text{m}$ counterparts are indicated by *open circles*. The $(R - K_s) \geq 5.3\text{mag}$ and $K_s < 20.2\text{mag}$ limits are shown as *solid horizontal* and *solid vertical* lines.

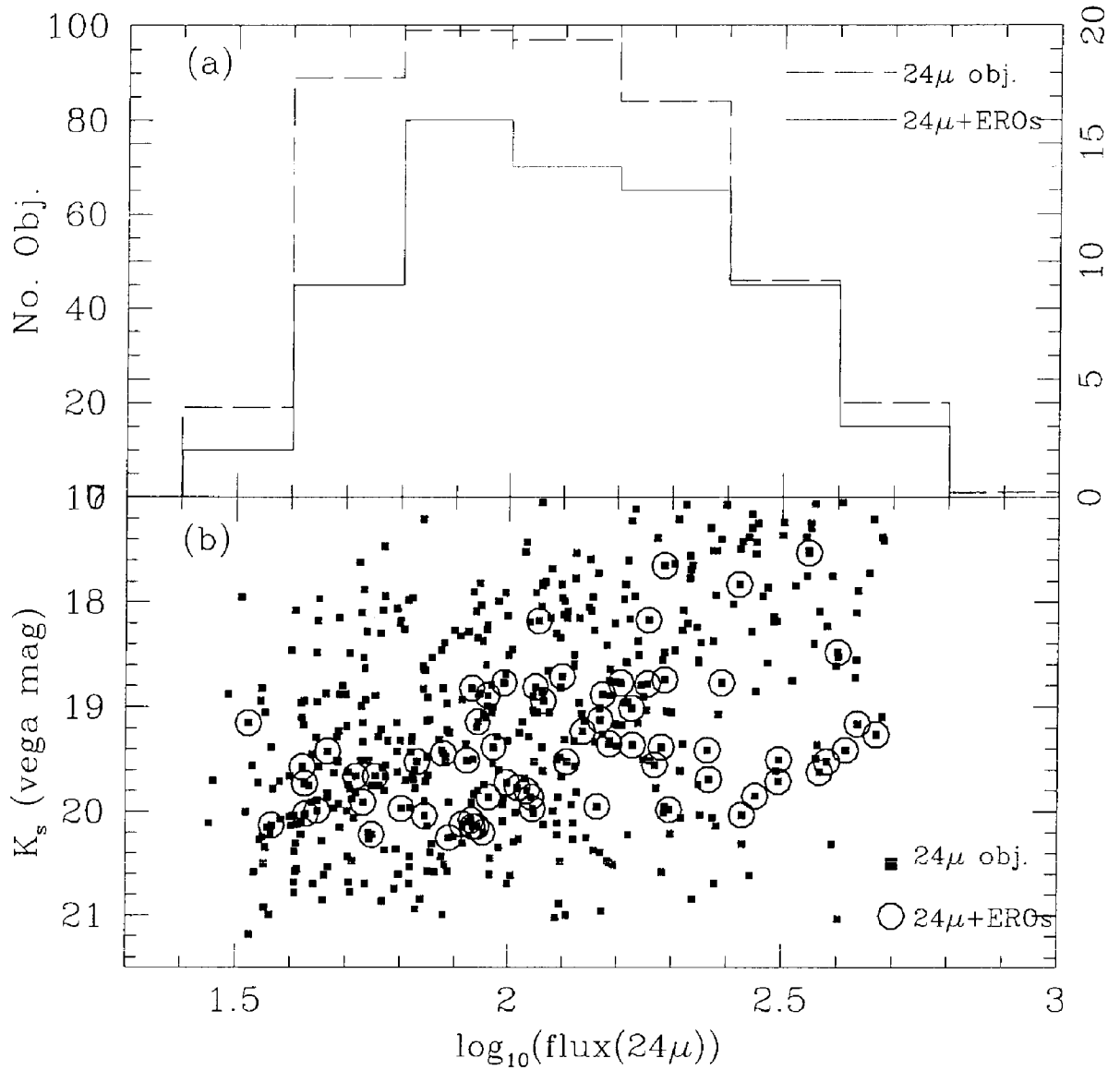


Fig. 2.— Panel 2a shows the $24\mu m$ flux distribution of the total (*dashed line*) and $24\mu m$ -detected ERO (*solid line*) populations. Panel 2b shows K_s vs. $24\mu m$ flux for all detected sources (*solid squares*) and for the EROs (*large open circles*).

3.2. The Nature of the EROs with $24\mu m$ Emission

What types of galaxies are the $24\mu m$ detected EROs? In Figure 3a, we present a 24 -to- $0.7\mu m$ and 24 -to- $2.2\mu m$ color-color diagram showing that $24\mu m$ -detected EROs (*red*

squares) are clearly separated from EROs without $24\mu\text{m}$ emission (*green points*), as well as the general non-ERO population (*black and blue*). This suggests that the MIR/Optical and MIR/NIR colors of $24\mu\text{m}$ -detected EROs are unique, distinguishing them from other populations. Figure 3b presents the expected colors as a function of redshift for various SED templates, assuming no evolution. The SEDs for M51 (normal spiral), M82 (starburst) and Mrk231 (dusty AGN) are taken from Silva et al. (1998), Fadda et al. (2002), and Chary & Elbaz (2001). In the case of M31's bulge (old stellar population), we use the near-IR J, H, K, IRAS 12, 25, 60 and $100\mu\text{m}$ fluxes, all within a $4'$ diameter aperture of the central nucleus (Soifer et al. 1986) and merge this with a 10 Gyr theoretical SED from Bruzual & Charlot.⁵ For comparison, a sample of 112, $24\mu\text{m}$ sources from the FLSV with known spectroscopic redshifts are marked to show the actual redshift range of the $24\mu\text{m}$ EROs in ELAIS N1. Of these 112 redshifts, 10 are $24\mu\text{m}$ -detected EROs with $0.8 < z_{\text{spec}} < 1.3$, and the optical spectra of these 10 sources all have [OII]3727Å emission line.

Comparing Figure 3a & 3b, we reach the following conclusions: 1) $24\mu\text{m}$ -detected EROs in the ELAIS N1 field with $(R - K_s) \geq 5.3\text{mag}$, $K_s < 20.2\text{mag}$, and $f_\nu(24\mu\text{m}) > 40\mu\text{Jy}$ are infrared bright sources at $z \geq 1$. They have colors similar to starbursts like M82 at $z \geq 1$, or dust reddened AGN like Mrk231 at $z \geq 0.7$. Their colors are too red to be explained by any normal spiral or old stellar populations at any redshifts. 2) The likely redshift range of these $24\mu\text{m}$ EROs is $z \geq 1$, as predicted from the model SEDs of M82 and Mrk231. This is further confirmed by comparison to the Keck spectroscopic sample from the FLSV. 3). The remaining half of the ERO population are probably galaxies with old stellar populations at $z \sim 1$, as suggested by the tracks in Figure 3b. In a forthcoming analysis, we should be able to set better constraints on the ages and masses of these systems by combining with the Spitzer IRAC photometry.

Half of the ELAIS N1 ERO sample have $24\mu\text{m}$ dust emission. The key question is what their infrared luminosities are. In the previous section, we conclude that the $24\mu\text{m}$ -detected EROs have colors similar to M82, however, Figure 3a does not set any constraints on either their luminosities or masses. We have a total of 112 redshifts for objects with $24\mu\text{m}$ counterparts (the FLSV 3σ flux limit is $90\mu\text{Jy}$). In Figure 4, we present the observed $24\mu\text{m}$ luminosity versus redshift for the spectroscopic FLSV sample. At $z \sim 1$ the observed $24\mu\text{m}$ luminosity roughly corresponds to the rest-frame IRAS $12\mu\text{m}$ luminosity, within a factor of 2. The Spitzer $24\mu\text{m}$ filter is narrower than the IRAS $12\mu\text{m}$ filter, but ignoring this difference, a crude conversion of the observed Spitzer $24\mu\text{m}$ flux can be made to place a lower limit on the rest-frame IRAS $12\mu\text{m}$ luminosity. We can infer the total infrared luminosity of

⁵<ftp://gemini.tuc.noao.edu/pub/charlot/bca5>

$24\mu m$ sources at $z \sim 1$ by using the correlation between the $12\mu m$ luminosity ($\nu L_\nu(12\mu m)$) and the infrared luminosity $L_{IR}(8 - 1000\mu m)$, $L_{IR} = 0.89 \times (\nu L_\nu(12\mu m))^{1.094} L_\odot$ (Soifer et al. 1989; Chary & Elbaz 2001). The mean flux ($167\mu Jy$) of the $24\mu m$ -detected EROs in ELAIS N1 implies the $L_{IR} \sim 3 \times 10^{11} L_\odot$ at $z = 1.0$ and $L_{IR} \sim 10^{12} L_\odot$ at $z = 1.5$, similar to that of local LIRGs and ULIGs. The corresponding SFR is $50 - 170 M_\odot/yr$, using $SFR = 1.71 \times 10^{-10} L_{IR}(M_\odot/yr)$ (Kennicutt 1998). We emphasize that the ELAIS N1 $24\mu m$ data is very deep so that 3σ flux limit of $40\mu Jy$ corresponds to a SFR of $12 M_\odot/yr$, which is more sensitive than the deepest 1.4GHz observation (Smail et al. 2002). In comparison, the SFR derived from the rest-frame [OII]3727Å emission line for EROs is roughly a few $\times M_\odot/yr$ (Yan, Thompson & Soifer 2004; Cimatti et al. 2003). Our SFR measurements are consistent with very deep measurements from the radio 1.4GHz (Smail et al. 2002). Using the evidence from both total infrared luminosity and colors, we conclude that $24\mu m$ detected EROs are dusty, infrared bright galaxies at $z \geq 1$, with total infrared luminosity on the order of $10^{11} L_\odot$ or larger.

3.3. Summary & Implications

Spitzer $24\mu m$ data in ELAIS N1 have revealed that $50 \pm 6\%$ of EROs with $(R - K_s) \geq 5.3\text{mag}$ and $K_s < 20.2\text{mag}$ have detectable $24\mu m$ emission above $40\mu Jy$. The colors and inferred redshifts of the $24\mu m$ -detected EROs suggest that they are infrared-luminous, dusty sources at $z \geq 1$. Their mean $24\mu m$ flux ($167\mu Jy$) corresponds to $\langle L_{IR} \rangle \sim 3 \times 10^{11} L_\odot$ at $z \sim 1$ and to $\langle L_{IR} \rangle \sim 10^{12} L_\odot$ at $z \sim 1.5$. Some of these $24\mu m$ -detected EROs could be AGN. The one mega-second Chandra observation in the HDF and optical spectroscopy suggest that the fraction of EROs likely to be AGN is small, around 10-20% (Alexander et al. 2002; Yan, Thompson & Soifer 2004). These dusty AGN can be identified when we combine this current analysis with the IRAC data. Our result suggests that a significant fraction of EROs are extremely active starbursts (LIRGs or ULIGs). If the time scale of this starbursting phase is on the order of $10^8/yr$, as inferred from local LIRGs and ULIGs (Sanders & Mirabel 1996), we can set a lower limit to the mass of these $24\mu m$ -detected EROs as $SFR \times \tau = 50 - 170 \times 10^8 = 5 \times 10^9 - 2 \times 10^{10} M_\odot$. If the EROs *without* detectable $24\mu m$ are indeed massive systems with old stellar populations at $z \sim 1$ as measured by several recent surveys (Glazebrook et al. 2004; Bell et al. 2003), one plausible connection between the starburst and early-type ERO populations is that the former may be in the process of transforming into the latter, as initially postulated by Kormendy & Sanders (1992). In the hierarchical clustering paradigm, it could be interpreted that our deep $24\mu m$ observations are capturing a massive galaxy population in the midst of violent transformation - possibly in the process of assembly via mergers/starbursts at the epoch of $z \sim 1 - 2$. The accurate

determination of the stellar and dynamical masses of these starburst EROs at $z \sim 1 - 2$ will be critical for the resolution of this question. Finally, the measurement of volume averaged mass density at $z \sim 1 - 2$ would require a better understanding of the physical source of the integrated K-band light — whether from dusty systems or from old stars.

Our result is consistent with what has been found with HST morphological studies of EROs. Yan & Thompson (2003) and Moustakas et al. (2004) have found that close to 50% of EROs with $K_s < 20$ have morphologies consistent with disk or later type galaxies in the observed 8100–8500 Å wavelength, and less than 40% show clean bulge type profiles. With the HST/ACS/NICMOS images in the FLSV region, we will be able to investigate the morphologies of these infrared luminous EROs, and to determine if indeed they are starbursting mergers at $z \sim 1$.

This work is based in part on observations made with the Spitzer Space Telescope, which is operated by the Jet Propulsion Laboratory, California Institute of Technology under NASA contract 1407. Support for this work was provided by NASA. The spectroscopic data presented herein were obtained at the W.M. Keck Observatory, which is operated as a scientific partnership among the California Institute of Technology, the University of California, and the National Aeronautics and Space Administration. The Observatory was made possible by the generous financial support of the W.M. Keck Foundation. We also wish to recognize and acknowledge the very significant cultural role and reverence that the summit of Mauna Kea has always had within the indigenous Hawaiian community. We are most fortunate to have the opportunity to conduct observations from this mountain.

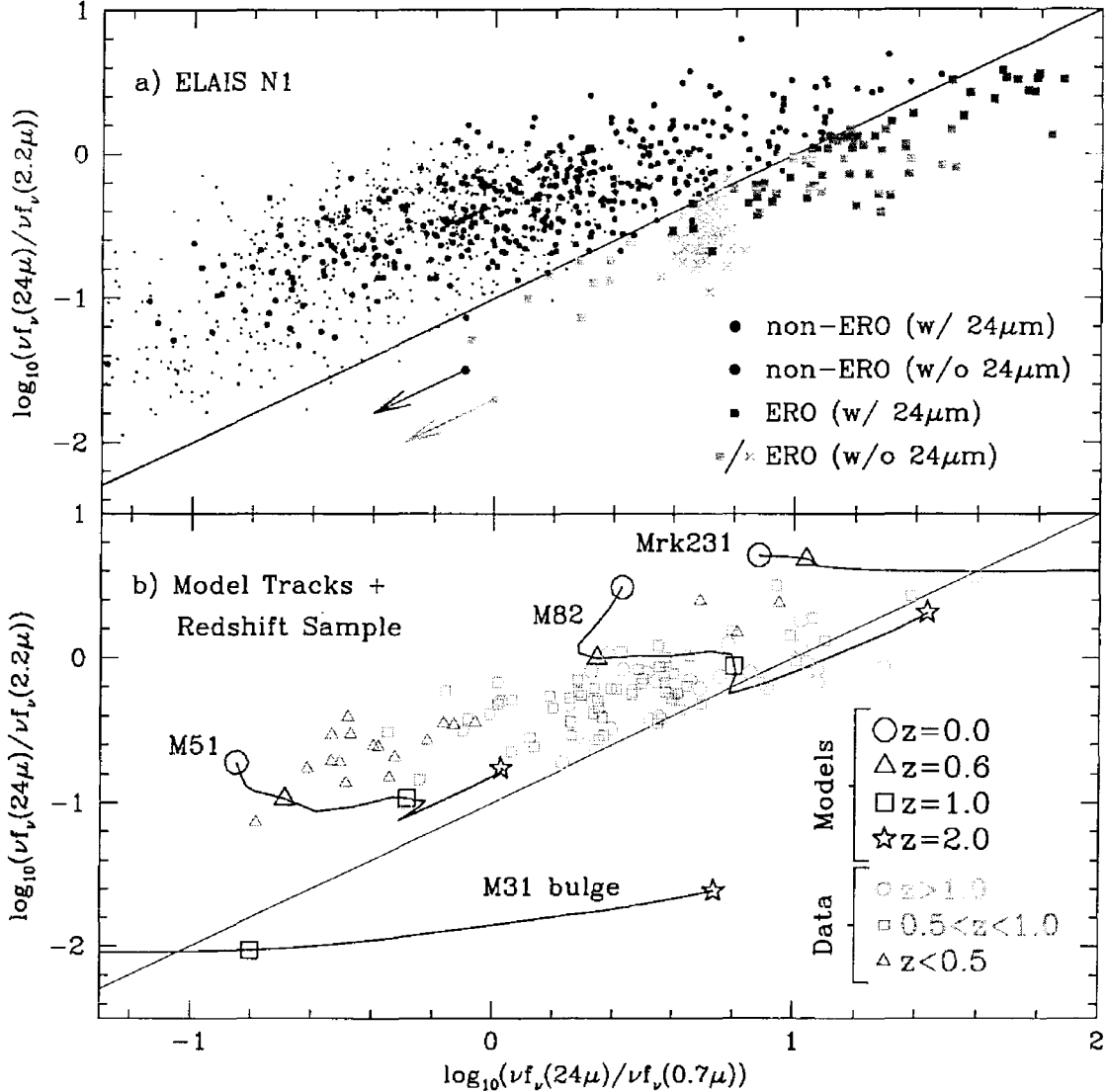


Fig. 3.— The two panels show $\log_{10}(\nu f_{\nu}(24\mu\text{m})/\nu f_{\nu}(0.7\mu\text{m}))$ versus $\log_{10}(\nu f_{\nu}(24\mu\text{m})/\nu f_{\nu}(8\mu\text{m}))$. **Panel 3a** presents the data from ELAIS N1. In this panel, *red/green squares* represent EROs with/without $24\mu\text{m}$ detections. For the non- $24\mu\text{m}$ EROs, the green crosses have only upper limits in the R -band. The *black/blue points* represent the full K_s -selected sample with/without $24\mu\text{m}$ detections. The plotted colors of sources not detected at $24\mu\text{m}$ are upper limits and could move down to lower-right corner of the diagram, as illustrated by the *green & blue arrows*. The *black solid line* in both panels represents constant $(R - K_s) = 5.3\text{mag}$ color. **Panel 3b** shows the computed color-color tracks as a function of redshift for a set of SED templates of local, well-known galaxies. The subset of the FLSV sample with measured spectroscopic redshifts are overplotted for three different redshift bins: $z < 0.5$ (*magenta open triangles*); $0.5 < z < 1.0$ (*orange open squares*); and $z > 1.0$ (*cyan open circles*).

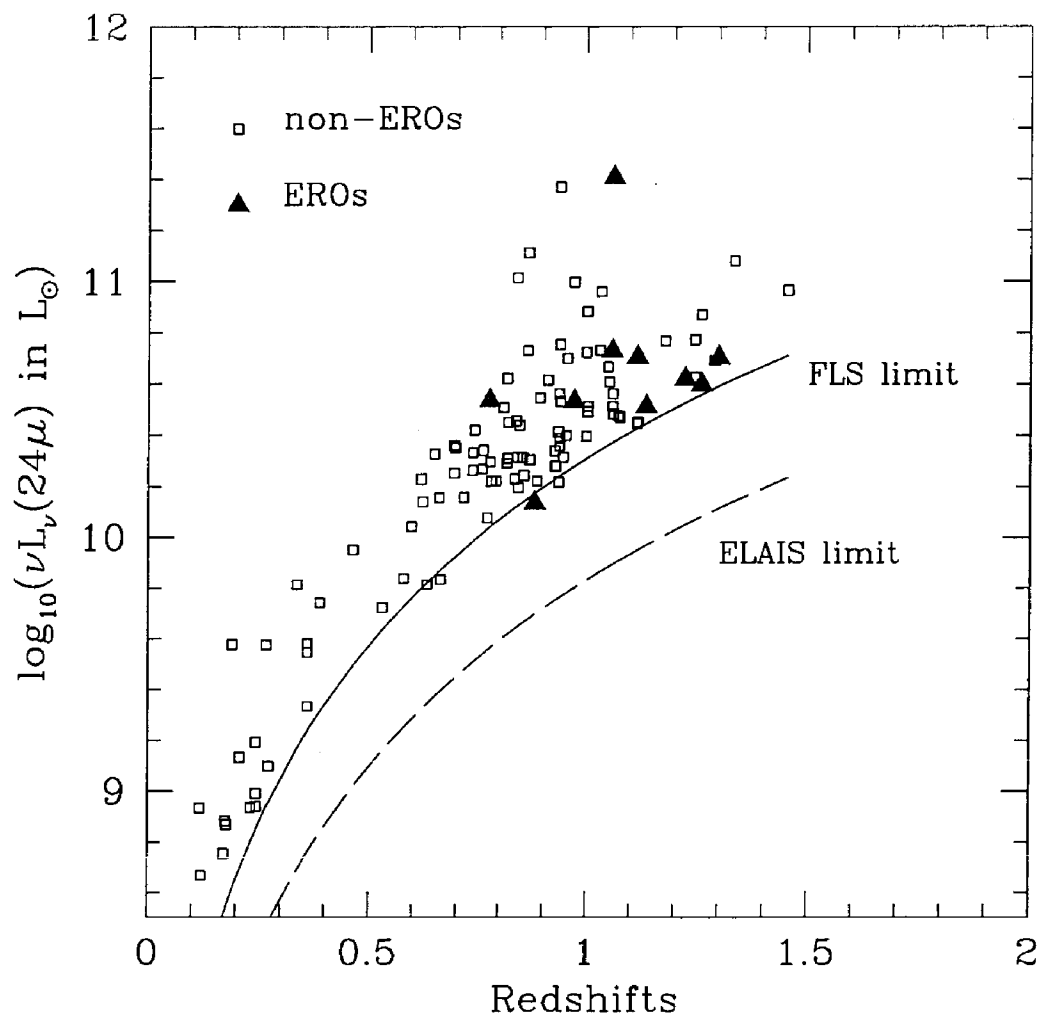


Fig. 4.— The observed $24\mu\text{m}$ luminosity as a function of spectroscopic redshift for a sample of 112 $24\mu\text{m}$ -detected sources in the FLSV region. The solid triangles are $24\mu\text{m}$ -detected EROs.

Table 1. Summary of Optical, NIR and $24\mu m$ Observations

Filter	<i>R</i>	<i>K_s</i>	$24\mu m$
FWHM (μ)	1.0	1.0	5.5
Pixel Scale (μ /pixel)	0.26	0.25	2.55
<Exp. Time> (sec)	1800	1800 ^a 9000 ^b	349 ^a 4268 ^b
3σ Limits	25.5 ^a 25.2 ^b	20.3 ^a 21.0 ^b	90 ^a 40 ^b
	mag	mag	μJy

^aFHSV

^bELAISN1

REFERENCES

- Alexander, D.M. et al. 2002, *AJ*, 123, 1149
- Bell, E. et al. 2003, *ApJS*, 149, 289
- Choi, P., et al. 2004, in prep.
- Daddi, E., et al. 2000, *A&A*, 361, 535
- Diolaiti, E.; et al. 2000, *A&A*, 147, 335
- Chary, R. & Elbaz, D. 2001, *ApJ*, 556 562
- Cimatti, A., et al. 2002, *A&A*, 381, 68
- Cimatti, Andrea; et al. 1998, *ApJ*, 499L, 21
- Dey, A. et al. 1999, *ApJ*, 519, 610
- Faber, S.M., et al. 2003, *SPIE*, 4841, 1657
- Fadda, D., Jannuzi, B., Ford, A., & Storrie-Lombardi, L.J., 2004, *AJ*, in press [astroph/0403490]
- Fadda, D. et al. 2004b, *ApJS*, in this volume.
- Glazebrook, K. et al. 2004, *ApJL*, in print. astroph/0401037
- Graham, J. & Dey, A. 1996, *ApJ*, 471, 720
- Hu, E.M., & Ridgway, S.E. 1994, *AJ*, 107, 1303
- Kormendy, J. & Sanders, D., 1992, *ApJL*, 390, 53
- Marleau, F. et al. 2004, *ApJS*, this volume.
- McCarthy, P.J., et al. 2001, *ApJ*, 560, L131
- McCarthy, P.J., 2004, *AR&AA*, 2004, submitted.
- McCarthy, P.J., Persson, S.E., West, S.C. 1992, *ApJ*, 386, 52
- Moustakas, L. et al. 2003, *ApJL*, in press
- Rieke, G. et al. 2004, in the same volume

- Roche, N.D., Almaini, O., Dunlop, J., Ivison, R.J., Willott, C.J. 2002, MNRAS, 337, 1282
- Sanders, D. & Mirabel, I.F. 1996, AR&A, 34, 749
- Silva, L., Granato, G.L., Bressan, A., Danese, L. 1998, ApJ, 509, 103
- Smail, I. et al. 2002, ApJ, 581, 844
- Soifer, B.T., et al. 1999, AJ, 118, 2065
- Soifer, B.T., Boehmer, L., Neugebauer, G., Sanders, D.B., 1989, AJ, 98, 766
- Soifer, B.T., et al. 1986, ApJ, 304, 651
- Werner, M. et al. 2004, in the same volume
- Yan, L. & Thompson, D.J. 2003, ApJ, 586, 765
- Yan, L., Thompson, D.J., & Soifer, B.T. 2004, AJ, 2004, 127, 1274